Virology 481 (2015) 151–160

Contents lists available at ScienceDirect

Virology

journal homepage: www.elsevier.com/locate/yviro

Molecular characterization of a novel hypovirus from the plant pathogenic fungus *Fusarium graminearum*

Pengfei Li, Hailong Zhang, Xiaoguang Chen, Dewen Qiu, Lihua Guo *

State Key Laboratory for Biology of Plant Disease and Insect Pests, Institute of Plant Protection, Chinese Academy of Agricultural Science, Beijing, China

ARTICLE INFO

Article history:
Received 17 December 2014
Returned to author for revisions
12 January 2015
Accepted 16 February 2015
Available online 14 March 2015

Keywords:
dsRNA
Mycovirus
Hypoviridae
Fusarium graminearum
Fusarium head blight
FgHV2

ABSTRACT

A novel mycovirus, termed Fusarium graminearum Hypovirus 2 (FgHV2/JS16), isolated from a plant pathogenic fungus, *Fusarium graminearum* strain JS16, was molecularly and biologically characterized. The genome of FgHV2/JS16 is 12,800 nucleotides (nts) long, excluding the poly (A) tail. This genome has only one large putative open reading frame, which encodes a polyprotein containing three normal functional domains, papain-like protease, RNA-dependent RNA polymerase, RNA helicase, and a novel domain with homologous bacterial SMC (structural maintenance of chromosomes) chromosome segregation proteins. A defective RNA segment that is 4553-nts long, excluding the poly (A) tail, was also detected in strain JS16. The polyprotein shared significant aa identities with Cryphonectria hypovirus 1 (CHV1) (16.8%) and CHV2 (16.2%). Phylogenetic analyses based on multiple alignments of the polyprotein clearly divided the members of *Hypoviridae* into two major groups, suggesting that FgHV2/JS16 was a novel hypovirus of a newly proposed genus-*Alphahypovirus*—composed of the members of Group 1, including CHV1, CHV2, FgHV1 and Sclerotinia sclerotiorum hypovirus 2. FgHV2/JS16 was shown to be associated with hypovirulence phenotypes according to comparisons of the biological properties shared between FgHV2/JS16-infected and FgHV2/JS16-free isogenic strains. Furthermore, we demonstrated that FgHV2/JS16 infection activated the RNA interference pathway in *Fusarium graminearum* by relative quantitative real time RT-PCR.

Introduction

Mycoviruses (fungal viruses) are viruses that infect and replicate in fungi (Ghabrial and Suzuki, 2009). Mycoviruses are widespread in the major taxonomic groups of fungi (Nuss, 2005; Ghabrial and Suzuki, 2009). Mycoviruses have three genomic types: single-stranded DNA (ssDNA) (Yu et al., 2010), double-stranded RNA (dsRNA) and single-stranded RNA (ssRNA). According to the ninth report of the International Committee on Taxonomy of Viruses (ICTV) (King et al., 2012), fungal viruses with ssRNA have been grouped into seven families: *Alphaflexiviridae*, *Gamaflexiviridae*, *Barnaviridae*, *Hypoviridae*, *Narnaviridae*, *Metaviridae* and *Pseudoviridae*. Research on mycoviruses has also been limited by lower levels of founding compared to viruses of other systems. However, several viruses can cause severe symptoms, such as changes in colony morphology, pigmentation, mycelial growth, sporulation, and virulence, including hypovirulence (Ghabrial and Suzuki, 2009). It is increasingly difficult to control diseases caused by plant pathogenic fungi via fungicides because the use of fungicidal sprays may lead to more fungicide-resistant fungal isolates (Ma et al., 2009; Gossen et al., 2001; Kuang et al., 2011) and may exert potential negative impacts on the environment as well as on food safety (Hu et al., 2014). Therefore, mycoviruses associated with hypovirulence can provide a potential route for the biological control of phytopathogenic fungal diseases (Chiba et al., 2009; Ghabrial and Suzuki, 2009).

Viruses of the family *Hypoviridae* have large ssRNA genomes that do not encode capsid proteins or produce true virions. Nine hypoviruses have been reported from five phytopathogenic fungi: *Cryphonectria parasitica*, *Sclerotinia sclerotiorum*, *F. graminearum*, *Valsa ceratosperma* and *Phomopsis longicolla*. Four confirmed virus species of the genus Hypovirus within the family *Hypoviridae* were isolated from *C. parasitica*: Cryphonectria hypovirus 1 (CHV1) (Hillman et al., 1990), CHV2 (Hillman et al., 1992, 1994), CHV3 (Smart et al., 1999), and CHV4 (Linder-Basso et al., 2005). Five unconfirmed viral species of the family *Hypoviridae* include Fusarium graminearum hypovirus 1 (FgHV1) (Wang et al., 2013), Phomopsis longicolla hypovirus 1 (PlHV1) (Koloniuk et al., 2014), Sclerotinia sclerotiorum hypovirus 1 (SsHV1) (Xie et al., 2011), SsHV2 (Khalifa and Pearson, 2014; Hu et al., 2014) and Valsa ceratosperma hypovirus 1 (VcHV1) (Yaegashi et al., 2012). Yaegashi et al. (2012) proposed that the family *Hypoviridae* contains two genera: *Alphahypovirus* and *Betahypovirus*. Hu et al. (2014) and Khalifa and Pearson (2014) suggested that a third distinct genus, *Gamahypovirus*, should be located in the family *Hypoviridae*: the genus *Alphahypovirus* contains three hypoviruses (CHV1, CHV2 and FgHV1),

* Corresponding author.
E-mail address: guolihua72@yahoo.com (L. Guo).

http://dx.doi.org/10.1016/j.virol.2015.02.047
0042-6822/

the genus *Betahypovirus* contains five members (CHV3, CHV4, SsHV1, VcHV1 and PlHV1) and the genus *Gammahypovirus* contains one hypovirus (SsHV2).

Fusarium head blight (FHB) is caused by *Fusarium* spp., which is a devastating disease with worldwide distribution that can completely destroy a potentially high-yielding crop within a few weeks of harvest (McMullen et al., 1997). Among the *Fusarium* species that cause FHB, *F. graminearum* is the predominant pathogen (Windels, 2000). *Fusarium graminearum* primarily infects wheat and barley and can result in a severe loss of grain yield as well as quality reduction. Mycotoxin contamination produced by *Fusarium* spp. may have a negative impact on both animal and human safety (O'Donnell et al., 2000; Rocha et al., 2005). To date, only a few mycoviruses were isolated from the phytopathogenic fungus *F. graminearum*: FgV1 (Fusarium graminearum virus 1), FgV2, FgV3, FgV4, FgV-ch9 and FgHV1/HN10 (Theisen et al., 2001; Chu et al., 2002; Yu et al., 2009; Darissa et al., 2011; Wang et al., 2013). Among them, FgV1 and FgV-ch9 were associated with the hypovirulence of *F. graminearum*. Therefore, it is urgent that new mycoviruses that significantly reduce host virulence should be exploited as alternative biological control agents of FHB.

In this study, we identified and characterized a novel mycovirus in the hypovirulent strain JS16 of *F. graminearum*. The new mycovirus is the second hypovirus from *F. graminearum*, and the effect of its infection on the biological properties of the host was also determined. In addition, the relative expression of several genes associated with RNA interference (RNAi) in fungi was determined by quantitative real-time reverse transcription PCR (qRT-PCR).

Results

Detection and sequencing of dsRNAs in F. graminearum strain JS16

The strain JS16 was identified as *F. graminearum* by polymerase chain reaction (PCR) amplification of the translation elongation factor (EF-1α) fragment (O'Donnell et al., 2000). DsRNA extracts from the mycelia of strain JS16 and virus-free strain JS16-F were treated with DNase I and S1 nuclease and were then subjected to 1% agarose gel electrophoresis. Two distinct dsRNA segments (L-dsRNA and S-dsRNA), which were approximately 13 kb and 5 kb, respectively, were observed in strain JS16, whereas the virus-free strain JS16-F did not contain any dsRNA segments (Fig. 1B). The two distinct dsRNA elements of strain JS16 were separately gel purified and used as templates for cDNA cloning.

The complete nucleotide sequence of the L-dsRNA segment, which is 12.8 kb, was determined by assembling the sequences of randomly primed cDNA, reverse transcription-polymerase chain reaction (RT-PCR), and Rapid Amplification of cDNA ends (RACE) clones. One-hundred and twenty-seven clones were obtained and were fully sequenced in both directions (data not shown). The full-length sequence of L-dsRNA was confirmed by RT-PCR with specific primers. The amplification of a specific PCR product using an oligo-dT primer revealed a poly (A) tail at the 3′ terminus of its plus strand. The complete genomic sequence (coding strand) was 12,800 nts long, excluding the poly (A) tail. To obtain the complete nucleotide sequence of the S-dsRNA, randomly primed cDNA was amplified by RT-PCR and cloned. Forty-six clones were obtained and were fully sequenced in both orientations (data not shown). The full-length sequence (coding strand) of the S-dsRNA that was 4553 nts long, excluding the poly (A) tail, was also confirmed by RT-PCR with specific primers.

Molecular characterization of FgHV2/JS16

A schematic representation of the genome organization of the coding strand of the L-dsRNA segment is shown in Fig. 1E. The genome contains a single long putative open reading frame (ORF) flanked by two untranslated regions (UTRs) at the 5′ and 3′ termini. The ORF, beginning at AUG (nt positions 458–460) and terminating at UAA (nt positions 12,290–12,292), was predicted to encode a polyprotein of 3944 amino acid (aa) residues, with a calculated molecular weight of 446.2 kDa. The deduced polyprotein contains three conserved domains of papain-like protease (Prot), RNA-dependent RNA polymerase (RdRp), and viral RNA helicase (Hel), which are contained in all of the members of the *Hypoviridae* family. The mycoviral L-dsRNA was tentatively assigned the name "Fusarium graminearum hypovirus 2 (FgHV2/JS16)". The sequence was deposited in GenBank under accession number KP208178. In addition, a novel domain that was similar to the bacterial chromosome segregation protein SMC (structural maintenance of chromosomes) was identified as being 293–543 aa downstream of the Prot domain (Fig. 1E) and had 8–17% sequence identity with the SMC domains reported from bacteria, archaea and eukaryotes, such as *Haladaptatus paucihalophilus* in archaea (*E*-value = 1*e* − 10; identities = 46/278 = 17%; Sequence ID: ref|WP_007975889.1) and *Gloeophyllum trabeum* ATCC 11539 in fungi (*E*-value = 1*e* − 09; identities = 33/276 = 12%; Sequence ID: ref|XP_007865850.1) and *Ruminococcus* sp. CAG:17 in bacteria (*E*-value = 2*e* − 09; identities = 26/243(11%); Sequence ID: ref|WP_021977666.1). We also found another five smaller ORFs (303–519 nt in length) on the plus and minus genomic strands. The predicted proteins of these small ORFs did not have any detectable similarity to the NCBI protein database (data not shown). Thus, these smaller ORF candidates were eliminated from further consideration.

The complete nt and polyprotein aa sequences of FgHV2/JS16 had the highest identity with CHV1/EP713, of 40.1% and 16.8%, respectively (Table 1). As previously described, stretches of the first and last 100 nts of the 5′-and 3′-UTRs showed significant conservation among hypoviruses in the same genus (Khalifa and Pearson, 2014). The full-length 5′-UTR (457 nt) of FgHV2/JS16 with multiple upstream AUG codons, similar to that found in CHV1/EP713, FgHV1/HN10 and SsHV2/5472, shared the highest identity (48%) with FgHV1/HN10 when using the first 100 nt of the 5′-UTR, while the 3′-UTR, which was 508 nt (excluding the poly (A) tail), shared the highest identity (41%) with VcHV1/MVC86 when using the last 100 nts of the 3′-UTR (excluding the poly (A) tail) (Table 1). In addition, the 5′-UTR had numerous and complex stem-loop secondary structures predicted using Mfold version 2.3 (Supplementary Fig. S1; Zuker, 2003). Sequence similarities among these hypoviruses showed that the L-dsRNA segment was the replicative form of an ssRNA mycovirus in the family *Hypoviridae*.

Molecular characterization of FgHV2/JS16 defective RNA (D-RNA)

The analysis of the complete sequence of S-dsRNA revealed it to be an FgHV2/JS16-derived D-RNA (Fig. 1E). Its sequence was deposited in GenBank under accession number KP208179. The sequence of D-RNA was composed of the 5′ terminal 1235 nts and 3′ terminal 3318 nts of FgHV2/JS16, of which the central region between nt positions 1236–9482 was deleted (Fig. 1E). RT-PCR of three primer pairs spanning the deletion region and northern blotting were performed to clarify whether D-RNA was derived from the genomic RNA (gRNA) of FgHV2/JS16 (Supplementary Tables S1 and S2). Three RT-PCR-amplified fragments derived from purified S-dsRNA were consistent with the genetic organization of D-RNA (Fig. 1C). In addition to the gRNA and D-RNA present in the total RNA extracts from strain JS16, no other bands that suggested subgenomic mRNAs (sgRNAs) were detected in the northern blot analysis using two probes specific to the 5′ and 3′ termini of FgHV2/JS16, respectively (Fig. 1D). Analysis of the genetic organization of D-RNA revealed a single putative ORF flanked by two 5′- and 3′-terminal untranslated regions (UTRs), which is consistent with the gRNA of FgHV2/JS16 (Fig. 1E). The ORF was predicted to encode a polyprotein of 1195 amino acid (aa) residues

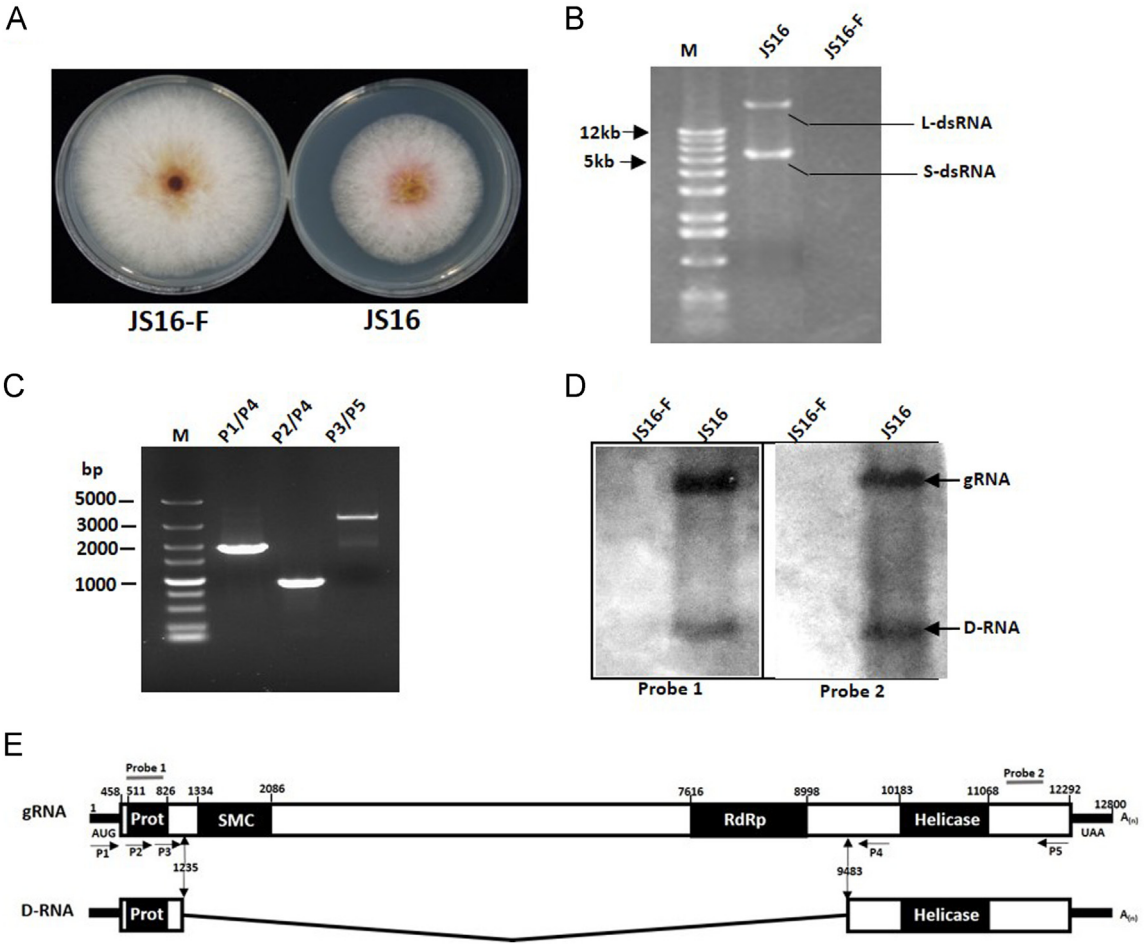

Fig. 1. (A) Colony morphology of strain JS16 and JS16-F (virus-free) after 4 d of culture on PDA in the dark. (B) dsRNA extraction of *F. graminearum* strains JS16 and JS16-F. The dsRNA fraction was electrophoresed in a 1% agarose gel and visualized under UV light after staining with ethidium bromide. Lane M, 1-kb DNA ladder marker. All of the samples were treated with DNase I and S1 nuclease. (C) Three RT-PCR-amplified fragments derived from FgHV2/JS16 D-RNA were subjected to 1% agarose gel electrophoresis. Lane M, 5-kb DNA marker. Lane P1/P4, RT-PCR-amplified products with primers 1 and 4. Lane P2/P4, RT-PCR-amplified products with primers 2 and 4. Lane P3/P5, RT-PCR-amplified products with primers 3 and 5. The locations of the five primers amplifying the three PCR fragments are shown in panel E. (D) Northern blotting detection of genomic RNA (gRNA) and defecting RNA (D-RNA) using digoxigenin-labeled probes 1 and 2. Probe 1 and probe 2 hybridized to both gRNA and D-RNA segments. The positions of these probes are indicated in panel E. (E) Schematic representation of the genomic organization of the virus gRNA and D-RNA. The open reading frame (458–12292 nt) of gRNA encodes a putative polyprotein containing four conserved domains, which are highlighted by shading in black: papain-like protease (Prot, 511–826 nt), chromosome segregation protein SMC (1334–2086 nt), RNA-dependent RNA polymerase (RdRp, 7616–8998 nt), and helicase (10,183–11,068 nt). The 5′-UTR (1–457 nt) and 3′-UTR (12,293–12,800 nt) are indicated with a thick line. The genome of D-RNA consists of the sequences of the 5′ and 3′ termini of gRNA. Compared with gRNA, D-RNA contains an 8247-nt deletion in the central portion (shown by a polygonal line). The open reading frame (458–4080 nt) of D-RNA encodes a putative viral protein containing two conserved domains, which are highlighted in blue: papain-like protease (Prot, 511–826 nt) and helicase (1931–2836 nt).

with a calculated molecular weight of 133.7 kDa, which was derived from a deletion between aa positions 259–3009, and a glycine substitution at aa position 260 of the gRNA-encoded polyprotein. Thus, the deduced polyprotein contained only two conserved domains, Prot and Hel, without the RdRp or SMC domains found in FgHV2/JS16 (Fig. 1E).

Phylogenetic relationships among FgHV2/JS16 and other hypoviruses

A putative Prot domain consisting of 105 aa was detected at the N-terminal end of the polyprotein of FgHV2/JS16 based on sequence alignment with other hypoviruses (Fig. 2A). It contained two strictly conserved aa residues (Cys^{26} and His^{83}), which were required for its autoproteolytic activity, as well as a glycine residue (Gly^{123}), which was associated with the potential cleavage site (Fig. 2A), similar to previously reported hypovirus proteases (Yuan and Hillman, 2001; Smart et al., 1999; Hillman et al., 1994; Koonin et al., 1991). The Prot domain of FgHV2/JS16 is closely related to that of FgHV1/HN10-B and CHV2/NB58, which have 18.7% and 13.3% aa sequence identity, respectively, based on multiple alignments of the Prot domains of all of the hypoviruses (Table 1). Phylogenetic analysis of the Prot domains using the maximum likelihood (ML) (Fig. 3A) and neighbor-joining (NJ) (Supplementary Fig. S2A) methods placed FgHV2/JS16 within the family *Hypoviridae*.

An RdRp domain was detected at aa positions 2387–2788 of the polyprotein. The FgHV2/JS16 RdRp contained all eight conserved motifs (Fig. 2B) that were found in the RdRp domains of other hypoviruses (Koonin et al., 1991). Although the SDD tripeptide was conserved among many hypoviruses (Yaegashi et al., 2012), the FgHV2/JS16 aa sequence contain a GDD tripeptide, which is found in several other newly identified hypoviruses, FgHV1/HN10, SsHV2/SX247 and SsHV2/5472, as well as in most ssRNA viruses (Wang et al., 2013; Hu et al., 2014; Khalifa and Pearson, 2014). The RdRp domain in FgHV2/JS16 has 29.4% amino acid sequence

Table 1
Sequence identities (%) between FgHV2/JS16 and other hypoviruses based on the multiple alignments of the complete nt sequence, the polyprotein sequence, the nt sequences of the 5′- and 3′-UTRs and the aa sequences of different domains.

Virus	Full sequence				Non-coding region				Coding region			GenBank accession no.[a]
	Complete seq.		ORFB		5′UTR[b]		3′UTR[b]		Pro	RdRp	Hel	
	Length (nt)	nt%	Length (aa)	aa%	Length (nt)	nt%	Length (nt)	nt%	aa%	aa%	aa%	
CHV1/EP713	12,712	40.1	3165[c]	16.8[c]	495	30.8	851	32.0	8.6/8.4[d]	29.4	23.0	M57938/ AAA67458
CHV2/NB58	12,507	38.8	3291[c]	16.2[c]	487	36.2	828	38.8	13.3	27.6	23.3	L29010/ AAA20137
CHV3/GH2	9799	31.6	2874	11.0	369	34.9	805	38.2	12.2	10.7	20.9	AF188515/ AAF13604
CHV4/SR2	9149	28.4	2848	11.3	193	42.7	409	29.0	11.4	10.5	21.6	AY307099/ AAQ76546
FgHV1/HN10	13,023	39.3	3705[c]	16.1[c]	510	48.0	480	39.4	9.5/18.7[d]	25.9	24.0	KC330231/ AGC75065
SsHV1/SZ-150	10,398	33.1	2948	10.9	541	40.2	1010	34.9	10.4	11.7	21.2	JF781304/ AEL99352
SsHV2/5472	14,581	35.8	4635	12.8	313	30.8	360	30.9	8.4	20.2	19.9	KF525367/ AHA56680
SsHV2/SX247	15,219	34.3	4699	11.8	467	32.7	654	31.1	7.6	20.7	20.5	KJ561218/ AIA61616
VcHV1/MVC86	9543	31.7	2940	10.8	378	39.2	342	41.0	9.5	11.7	20.3	AB690372/ BAM08994
PlHV1/ME711	9760	31.7	2848	11.3	732	37.9	904	40.4	8.4	10.7	22.9	KF537784/ AIG94930

[a] Complete sequence (nt/aa) accession numbers.
[b] The terminal 100 nt of the 5′- and 3′-UTR sequences were compared to the respective UTR of each virus.
[c] aa sequence of ORF B was used.
[d] Identities to Prot domains of ORF A and ORF B are separated by a slash.

Fig. 2. Amino acid sequence alignment of the putative Prot (A), RdRp (B) and Hel (C) domains of FgHV2/JS16 and those of selected viruses in the family of *Hypoviridae*, including FgV1/DK21 and PPV. Identical residues are shaded. Asterisks and dots indicate identical amino acid residues and similar amino acid residues, respectively.

identity with CHV1/EP713 and 27.6% identity with CHV2/NB58 (Table 1). Phylogenetic trees based on the RdRp domains using the ML (Fig. 3B) and NJ (Supplementary Fig. S2B) methods clearly placed FgHV2/JS16 between the FgHV1 and SsHV2 branches.

A Hel domain was identified at the C-terminal end of the polyprotein of FgHV2/JS16, 3243–3538 aa downstream from the RdRp domain, and contained three conserved motifs: a GKST box, a DExH box and a QRxGR box, as previously described in other hypoviruses (Fig. 2C). Notably, the fourth amino acid of the GKST box was replaced by a Ser residue, similar to FgHV1/HN10, SsHV2/5472 and SsHV2/SX247, and the second and fourth amino acids of the QRxGR box were replaced by glycine and alanine residues, respectively. The Hel domain encoded by FgHV2/JS16 was closely related to that of FgHV1/HN10, CHV2/NB58 and CHV1/EP713, with 24.0%, 23.3% and 23.0% aa identity, respectively (Table 1). Phylogenetic trees based on the Hel domains using the ML (Fig. 3C) and NJ methods (Supplementary Fig. S2C) clustered FgHV2/JS16 with, but distinctly branched from, the clade including CHV1, CHV2, FgHV1 and SsHV2.

Phylogenetic analyses of the viral polyproteins using the ML (Fig. 3D) and NJ (Supplementary Fig. S2D) methods placed FgHV2/JS16 between the FgHV1 and SsHV2 branches and also clearly

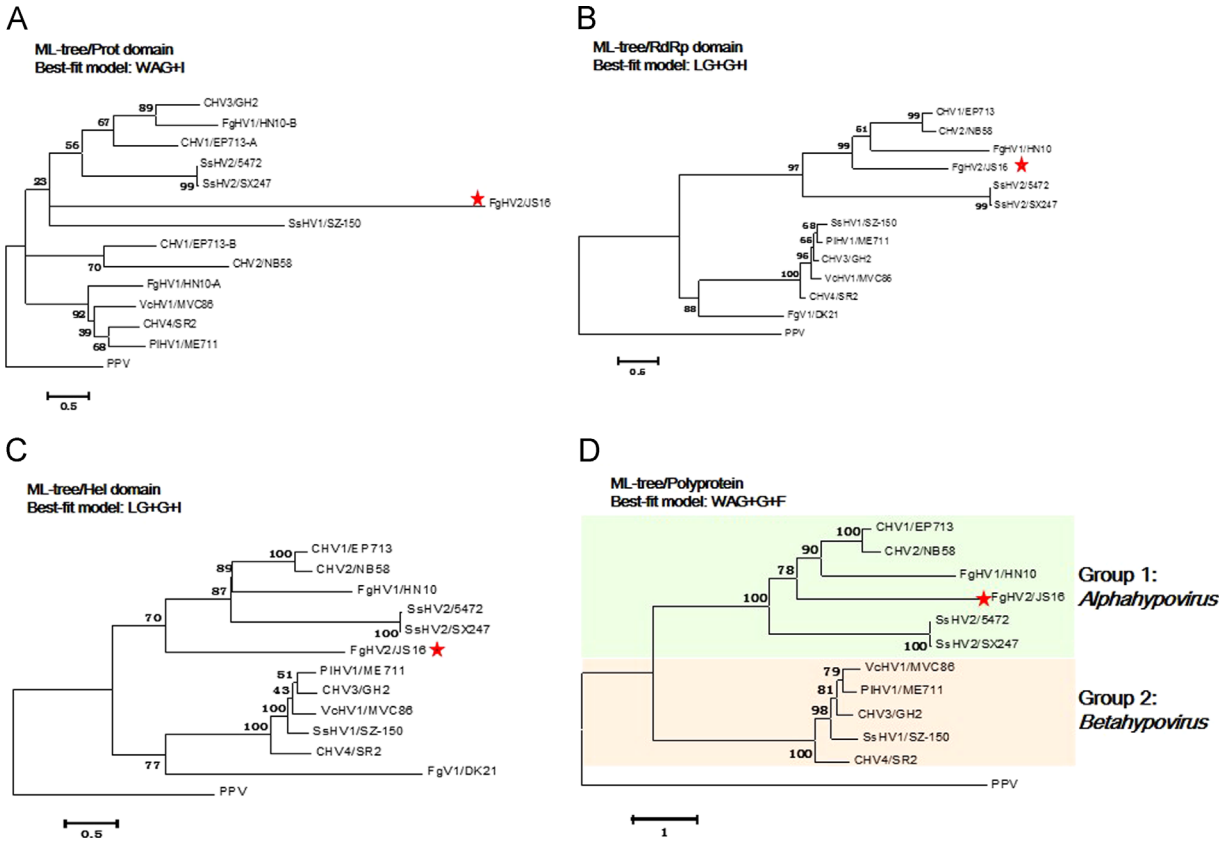

Fig. 3. Maximum likelihood phylogenetic trees based on multiple alignments of the Prot (A), RdRp (B) and Hel domains (C) as well as polyproteins (D) of FgHV2/JS16 and other *Hypoviridae* members. All of the approved and probable hypoviruses were placed in two lineages (*Alphahypvirus* and *Betahypovirus*) based on phylogenetic analyses of the RdRp, Helicase domains and polyproteins. The scale bar at the lower left represents a genetic distance. Plum pox virus (PPV) was used as an out-group.

divided the members of *Hypoviridae* into two major groups: Group 1 (CHV1, CHV2, FgHV1, FgHV2 and SsHV2) and Group 2 (SsHV1, PIHV1, CHV3, VcHV1 and CHV4), which is consistent with a phylogenetic analysis based on both the RdRp and Hel domains in the family *Hypoviridae*. In Group 1, the FgHV2/JS16 polyprotein shared 16.1–16.8% identity with CHV1, CHV2 and FgHV1 (the previously proposed *Alphahypovirus* members) and had a lower identity (11.8–12.8%) with SsHV2 (the previously proposed *Gammahypovirus* members) (Table 1).

Biological effects of FgHV2/JS16 on F. graminearum

To assess the effect of FgHV2/JS16 infection on the biological properties of *F. graminearum* strain JS16, a virus-free strain was required. To eliminate FgHV2 from strain JS16, we used many methods, including single conidial isolation and protoplast-regenerant isolation. In all, 493 isolates were detected as virus-positive. By a combination of protoplast-regenerant and Ribavirin treatment, one strain (JS16-F) was cured of FgHV2/JS16. By single ascospore isolation, the strain JS16-F2 was one of five strains confirmed to be cured of FgHV2/JS16, as determined by dsRNA extraction, RT-PCR and northern dot blot (data not shown). Compared to the virus-free strain JS16-F, strain JS16 showed abnormal colony morphology (Fig. 1A). Strain JS16 grew on potato dextrose agar (PDA) medium at a rate of 7.5 mm/day, which was 16.0% slower than the growth of strain JS16-F (9.0 mm/day) (Fig. 4B). In addition, strain JS16 had a significant reduction in colony diameter (33.1% reduction, $p < 0.01$) (Fig. 4A), biomass (47.1% reduction, $p < 0.01$) (Fig. 4C), conidia production (70.7% reduction, $p < 0.01$) (Fig. 4D) and DON concentration (77.4% reduction, $p < 0.01$) (Fig. 4E). In the virulence assay, the virus-free strain JS16-F spread more quickly from the inoculation sites to nearby spikelets than the virus-carrying strain JS16. At 14 d post-inoculation, there was a significant difference in the numbers of diseased spikelets per invaded wheat head (44.6% reduction, $p < 0.01$) (Fig. 4F). Fusarium head blight symptoms and kernel quality after the infection of wheat spikes with *F. graminearum* strain JS16 and JS16-F were also photographed (Fig. 4G and H). A similar trend was confirmed in the same characteristics between strains JS16 and JS16-F2, which is a cured strain by single ascospore isolation, as confirmed between strains JS16 and JS16-F (data not shown). Thus, FgHV2/JS16 infection had significant effects on fungal phenotypes.

Expression of the genes involved in PTGS by relative quantitative real time RT-PCR

To examine the gene expression of strain JS16 in response to FgHV2/JS16 infection, we identified 9 *F. graminearum* genes involved in PTGS based on the *C. parasitica* Dicer, Argonaute and RNA-dependent RNA polymerase (RdRP) gene sequences, extracted total RNA from the mycelial mass of strain JS16 and strain JS16-F and determined their relative expression by quantitative real-time RT-PCR (qRT-PCR). As shown in Fig. 5, of the 2 Argonaute-like genes designated *agl1* and *agl2*, the expression of FGSG_08752 (*agl1*) was significantly up-regulated at both 36 h and 5 d in FgHV2-infected JS16 relative to virus free JS16. Of the 2 Dicer-like genes designated *dcl1* and *dcl2*, the expression of FGSG_04408 (*dcl2*) was strongly up-regulated at both 36 h and 5 d. Of the 5 RdRP-like genes designated *rdr1-rdr5*, the expression of FGSG_01582 (*rdr4*) was also strongly up-regulated at both 36 h and 5 d. The expression of FGSG_08752 (*agl1*) and FGSG_04408 (*dcl2*) at 5 d was more strongly up-regulated than that at 36 h, whereas the expression of FGSG_01582

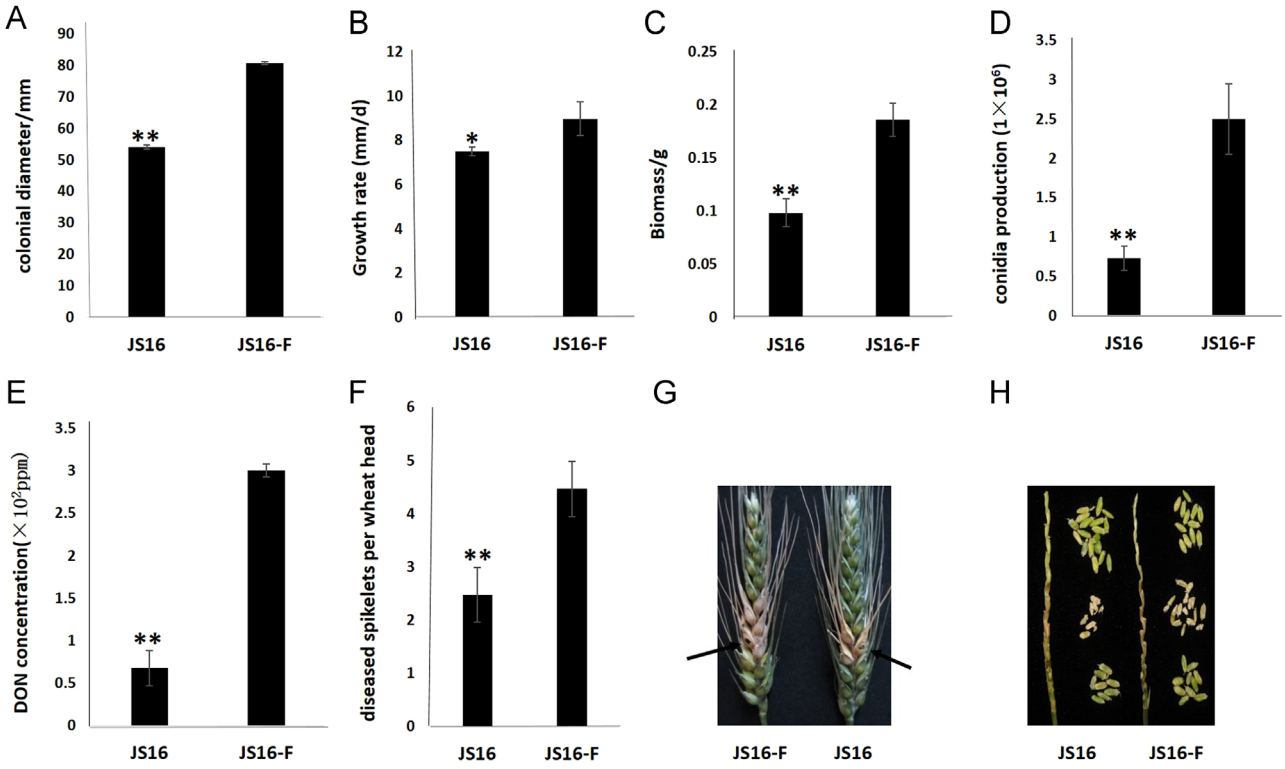

Fig. 4. Biological impact of FgHV2/JS16 infection on *F. graminearum*. (A) Comparison of the colony diameter between JS16 and JS16-F. (B) Growth rate after 4 d on PDA. (C) Biomass comparison of strain JS16 and JS16-F. (D) Conidial production after 5 d in CMC liquid medium. (E) Mycotoxin DON production on wheat grain by virus-free and virus-carrying fungal strains 14 d post-inoculation. (F) The virulence on wheat grain of strain JS16 and JS16-F 14 d post-inoculation was assessed by the numbers of diseased spikelets per wheat head invaded. (G) Fusarium head blight symptoms caused by virus-free and virus-carrying fungi in the fields. The black dots and arrows indicate the inoculation positions. Pathogenicity tests were repeated at least 15 times for every strain. (H) Kernel quality after infection of wheat spikes with *F. graminearum* strain JS16 and JS16-F. Kernels represent the original position at the spike before harvesting and the yield of one spike 2 weeks post-infection in the fields. The bars (A–H) represent the standard deviations from the mean ($n=3$). "*" indicates that differences are statistically significant ($p<0.05$). "**" indicates a significant difference ($p<0.01$).

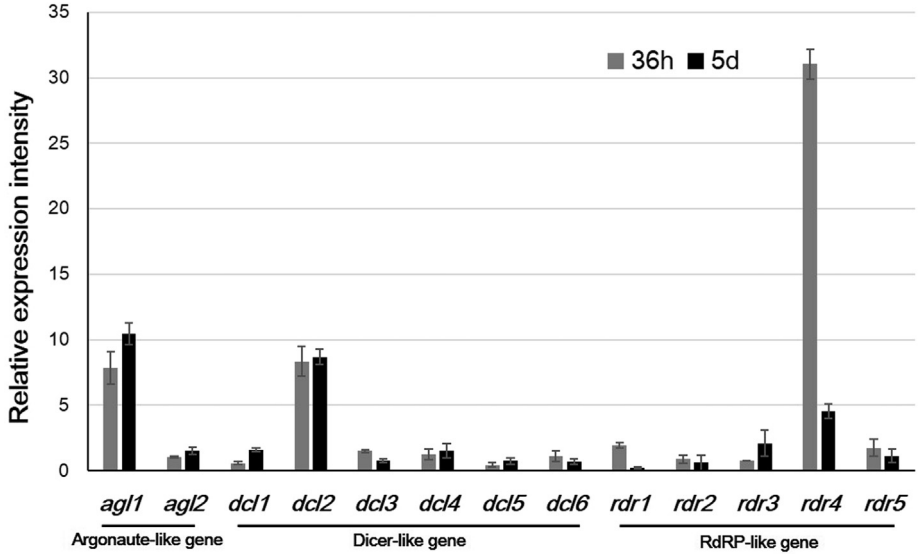

Fig. 5. The expression of the genes involved in PTGS by relative quantitative real-time RT-PCR. The expression of the selected genes at 36 h and 5 d are indicated by gray and black bars, respectively. Nine *F. graminearum* genes involved in PTGS were identified based on the *C. parasitica* Dicer, Argonaute and RdRP gene sequences. Of them, two Argonaute-like genes (FGSG_08752 and FGSG_00348) are designated *agl1* and *agl2*, two Dicer-like genes (FGSG_09025, FGSG_04408, are designated *dcl1-dcl6*, and five RdRP-like genes (FGSG_04619, FGSG_06504, FGSG_08716, FGSG_01582, FGSG_09076) are designated *rdr1-rdr5,* respectively.

(*rdr4*) was far more strongly up-regulated at 36 h than that at 5 d (Fig. 5). By contrast, some genes, such as FGSG_06504 (*rdr2*) were down-regulated at both 36 h and 5 d in FgHV2-infected JS16 relative to virus free JS16.

Discussion

In this study, we described the molecular and biological characterization of a novel mycovirus, FgHV2/JS16, which infected

the plant pathogenic fungus Nine *F. graminearum*. The full-length sequence of FgHV2/JS16 is 12,800 nts, excluding the poly (A) tail. The genome contains a single ORF encoding a polyprotein of 3944 amino acid residues with a calculated molecular mass of 446.2 kDa. A homology search and sequence alignment revealed that FgHV2/JS16 was closely related to members of the family *Hypoviridae*.

To date, there are three suggested genera in the family *Hypoviridae*, *Alphahypovirus* (CHV1, CHV2 and FgHV1), *Betahypovirus* (CHV3, CHV4, PIHV1, SsHV1 and VcHV1) and *Gammahypovirus* (SsHV2) (Yaegashi et al., 2012; Khalifa and Pearson, 2014; Hu et al., 2014). Generally, the genomes of viruses in the *Alphahypovirus* genus consist of two ORFs; ORF B only contains three conserved domains: Prot, RdRp and Hel. The genomes of viruses in the *Betahypovirus* genus consist of a single ORF encoding a single polyprotein with four conserved domains: Prot, RdRp, Hel and UDP-glucosyltransferase (UGT) (Khalifa and Pearson, 2014). The genomes of viruses in the genus *Gammahypovirus* consist of a single ORF that encodes a single polyprotein with three conserved domains: Prot, RdRp and Hel. As previously described, the genomes of *Alphahypovirus* and *Betahypovirus* range from 9 to 13 kb in size (Wang et al., 2013; Dawe and Nuss, 2013; Yaegashi et al., 2012; Khalifa and Pearson, 2014; Hu et al., 2014). In terms of our results, the genome size of FgHV2/JS16 is 12.8 kb, and the sequence alignments based on the complete nt sequence, the polyprotein sequence and the aa sequence of the conserved domains (Prot, RdRp and Hel) suggest that FgHV2/JS16 is closely related to the viruses of the genus *Alphahypovirus,* as SsHV2 was described. In addition, phylogenetic analyses based on the polyprotein and conserved domains (RdRp and Hel) using ML and NJ methods clearly divided the members of *Hypoviridae* into two major groups: Group 1 (including FgHV2 and members of *Alphahypovirus* and *Gammahypovirus*) and Group 2 (including *Betahypovirus* members), although the genomic organization of FgHV2/JS16 is obviously different from that of the *Alphahypovirus* members, whereas it is similar to that of the members of the *Gammahypovirus genus*. Therefore, we suggest that the members (CHV1, CHV2, FgHV1, FgHV2 and SsHV2) of Group 1 constitute the same genus, *Alphahypovirus*, with the FgHV2/JS16 as a new member of this newly proposed genus, while the members (CHV3, CHV4, PIHV1, SsHV1 and VcHV1) of Group 2 constitute the same genus, *Betahypovirus* (Fig. 3D; Supplementary Fig. S2D). Based on the analysis above, we conclude that the evolution of viruses in the family *Hypoviridae* is very complex. As an increasing number of hypoviruses are discovered, we will better understand the ecology and evolutionary complexity of hypoviruses.

Wang et al. (2013) suggested that there is gene flow between the *Alphahypovirus* and *Betahypovirus* genera in the family *Hypoviridae*. Recombination analysis using RDP4.39 (Martin et al., 2010) revealed 20 recombination events in the family *Hypoviridae* (Supplementary Table S3; Supplementary Figs. S3 and S4), which support the viewpoint of Wang et al. (2013). Of the 20 predicted recombination events, 13 were predicted to have major and minor parents from the *Alpha–Betahypovirus* genera, suggesting that gene flow between the *Alpha–Betahypovirus* genera may be a driving force in the evolutionary history of hypoviruses. In addition, the fact that both FgHV1/HN10 and PIHV1/ME711 were identified as most major parents, while CHV2/NB58 was identified as most minor parents by RDP4.39 (Figs. S3 and S4), provides the possibility that FgHV1/HN10, PIHV1/ME711 and CHV2/NB58 or their ancestors have a long evolutionary history. In FgHV2/JS16, three out of five recombination events were predicted to have major and minor parents from the *Alphahypovirus* and *Betahypovirus* genera, and another two recombination events had the same major and minor parent from FgHV1/HN10 and CHV2/NB58, suggesting that FgHV2/JS16 is a complex recombinant.

A D-RNA segment derived from the genomic RNA of FgHV2 was also detected in JS16 and was completely sequenced. D-RNA and defective interfering RNA (DI-RNA) are forms of subviral RNAs that are found in many RNA viruses, and D-RNA or DI-RNA has closely related, shorter segments of parental viral RNAs that usually encode truncated, defective proteins or no proteins (Chiba et al., 2013). D-RNAs have been described in hypoviruses with ssRNA genomes, including CHV1 and CHV3 (Hillman et al., 2000; Hillman and Suzuki, 2004; Shapira et al., 1991; Suzuki et al., 2003). FgHV2 D-RNA is similar in structure to CHV3 D-RNA: a single major ORF can be detected from the deduced translations of the D-RNA, and the 5′ terminal section that contains the complete putative protease of genomic RNA is fused in-frame to the 3′ terminal section that contains the complete putative helicase of genomic RNA (Hillman et al., 2000). How the structure of these two D-RNAs is generated and whether this structure provides advantages to defective molecules are still unknown. In the case of CHV1, defective RNAs significantly contribute to the complexity of the dsRNA populations found in hypovirulent strains of *C. parasitica* (Shapira et al., 1991), and the generation of D-RNAs in fungi is dependent on host RNA silencing pathways (Zhang and Nuss, 2008). As Chiba et al. (2013) reported, DI-RNAs of Rosellinia necatrix partitivirus 2 (RnPV2) can affect the replication of its parental virus and reduce viral symptom expression in a Dicer-like 2 knockout mutant of *C. parasitica* (chestnut blight fungus), which is an artificial host for RnVP2. Therefore, the discovery of D-RNAs in JS16 infected with FgHV2 is of great significance. Similar to CHV1 and CHV3, whether FgHV2/JS16 D-RNA affects viral replication and the fungal host phenotype is unknown. Therefore, further research is required to clarify these issues.

A novel domain, the bacterial SMC domain, was detected in the polyprotein of FgHV2/JS16, which had weak similarities to those reported in bacteria, archaea, and eukaryotes. SMC proteins have five recognizable domains: amino- and carboxy-terminal globular domains, two coiled-coil regions separating the terminal domains, and a central flexible hinge (Harvey et al., 2002). Amino acid sequence alignment of the putative SMC domain of FgHV2/JS16 and those of selected bacterium and archaea show that the SMC domain of FgHV2/JS16 is localized to the carboxy-terminal coiled-coil region separating the globular ends that are capable of binding DNA (Supplementary Fig. S5). Because of weak similarities to those reported in bacteria, archaea, and eukaryotes, the SMC domain of FgHV2/JS16 form a distinct branch from those of selected bacterium and archaea (Supplementary Fig. S6). SMC proteins play a crucial role in chromosome segregation, chromosome-wide gene regulation and recombinational repair (Hirano, 2006). SMC proteins are also essential for genome integrity and are key organizers of chromosome architecture in bacteria, archaea, and eukaryotes (Laflamme et al., 2014; Soppa et al., 2002; Haering et al., 2002; Jensen and Shapiro, 2003). The coiled-coil regions of bovine SMC3 protein are proved to have the ability alone to bind DNA (Akhmedov et al., 1999). The coiled-coil domains of yeast SMC5 protein contain most of the microtubule-binding sites and SMC–microtubule interactions are essential to establish a robust system for maintaining genome integrity (Laflamme et al., 2014). SMC1 of the host cell plays a key role in the DNA replication of the minute virus of canines, a member of the family *Parvoviridae* and genus *Bocavirus* (Luo et al., 2013). To date, the only example of an SMC domain in a eukaryotic virus is from Lygus lineolaris virus 1, which infects the tarnished plant bug (Perera et al., 2012). FgHV2/JS16 is the second eukaryotic virus to express a putative SMC domain protein and the first fungal virus to do so. Therefore, it would be interesting to undertake further research to investigate the function of the SMC domain of FgHV2/JS16 on binding DNA or microtubule and the effect of the SMC domain of the host fungi on FgHV2/JS16 replication. The existence of a bacterial-type SMC

domain in a mycovirus may suggest horizontal gene transfer and recombination between viruses, bacteria and eukaryotes.

As previously reported, the expression of genes involved in dsRNA-mediated gene silencing is strongly induced in response to viral infection (Zhang et al., 2008; Lee et al., 2014). Thirteen *F. graminearum* genes responsible for PTGS were selected to examine the effect of FgHV2/JS16 on the expression of these genes. An Argonaute-like gene (FGSG_08752, *agl1*), a Dicer-like gene (FGSG_04408, *dcl2*), and an RdRP-like gene (FGSG_01582, *rdr4*) were significantly up-regulated at both 36 h and 5 d, indicating that these genes may play an important role in gene silencing. As previously described, a single Dicer protein, DCL2, and a single Argonaute protein, AGL2, were shown to serve as effective antiviral defense responses in the chestnut blight fungus *C. parasitica* (Segers et al., 2007; Sun et al., 2009; Zhang et al., 2014), whereas the *C. parasitica* RdRP genes are not required for the antiviral defense response (Zhang et al., 2014). However, the roles of the RdRP genes in antiviral PTGS in the *F. graminearum* have not been characterized. Therefore, it is necessary to investigate the function of the RNAi genes that are involved in the response of *F. graminearum* to mycovirus infection and to study the interaction between mycoviruses and their host fungi.

In many cases, such as CHV4 (Linder-Basso et al., 2005) and FgHV1/HN10 (Wang et al., 2013), viral infection is not associated with phenotypic changes. However, CHV1/EP713, CHV2/NB58 and SsHV2/SZ247 can confer hypovirulence to their host fungi. Strain JS16 is a hypovirulent strain and exhibits dramatic phenotypes, including a reduced mycelial growth rate, conidia production and deoxynivalenol (DON) concentration. Therefore, as a hypovirulent mycovirus, FgHV2/JS16 may potentially be useful for disease biocontrol, similar to the case of CHV1/EP713, which is used against chestnut blight (Nuss, 2005).

Materials and methods

Fungal isolates and culture conditions

Fusarium graminearum strain JS16 was isolated from the diseased glumes of wheat infected with *Fusarium* spp. collected in the Jiangsu province of China. Strain JS16-F was a virus-free strain derived from strain JS16 treated with 80–100 μM concentrations of Ribavirin (Herrero et al., 2011). Strain JS16-F2 was another virus-free strain derived from isogenic strain JS16 by single ascospore isolation. All of the *F. graminearum* isolates were maintained on potato dextrose agar (PDA) at 25 °C in the dark. Mycelial agar discs were stored in a sterilized 25% glycerol solution at −80 °C.

dsRNA detection and purification

Mycelial plugs of strain JS16 were cultured on PDA plates overlaid with cellophane membranes for 4 d at 25 °C in the dark. The mycelial mass was collected and ground in liquid nitrogen with a mortar and pestle to a fine powder. DsRNA was extracted by the CF-11 cellulose (Sigma-Aldrich, Dorset, England) chromatography method, as previously described (Valverde, 1990). Total nucleic acid was digested with DNase I and S1 nuclease (TaKaRa Bio Inc., Dalian,China) following the manufacturer's instructions. The final dsRNA fraction was electrophoresed in a 1% agarose gel and the dsRNA was visualized by staining with ethidium bromide.

Northern blot analysis

Northern hybridization was performed to verify the existence of D-RNA in strain JS16. The total nucleic acids from 1 mg of the mycelia of isolate JS16 were separated on 1% agarose gel in 1 × TAE buffer (40 mM Tris-acetate, 1 mM EDTA, pH 8.0) under denaturing conditions. The RNAs were denatured by the addition of 7.8 μl of RNA buffer (1 μl of 10 × MOPS, 5 μl of formamide, 1.8 μl of formaldehyde solution) and heating at 68 °C for 10 min. The nucleic acids were then transferred onto Hybond-N^+ nylon membranes (Amersham Biosciences, Buckingham, England) by capillary blotting with 20 × SSC (3 M NaCl, 0.3 M sodium citrate, pH 7.0) overnight. The RNAs were cross-linked to the membrane by UV irradiation for 10 min. The DNA probes specific for RNAs were digoxigenin (DIG)-11-dUTP-labeled DNA fragments that were amplified by PCR as recommended by the manufacturer (Roche Diagnostics, Mannheim, Germany). Chemiluminescent signals of the probe-RNA hybrids were detected with a DIG detection kit (Roche).

Molecular cloning and sequencing

The cDNA synthesis and sequencing of dsRNAs were conducted as previously described (Wang et al., 2013; Xie et al., 2011). cDNAs of the purified dsRNA isolated from strain JS16 were synthesized by RT-PCR. Approximately 7 μl of dsRNA was mixed with the tagged random primer-dN6 (5′-GACGTCCAGATCGCGAATTCNNNNNN-3′), denatured at 95 °C for 10 min and immediately chilled on ice for 5 min. dsRNA was reverse transcribed in a reaction mixture using M-MLV Reverse Transcriptase (Promega) according to the manufacturer's instructions. Random cDNA amplifications were carried out using a specific primer (5′-GACGTCCAGATCGCGAATTC-3′) based on the tagged random primer-dN6 and PrimeSTAR® HSDNA Polymerase (TaKaRa) on a Thermal Cycler (Bio-Rad, Hercules, CA, USA). The amplified PCR products were purified using an EasyPure Quick Gel Extraction Kit (TransGen). The products were cloned with a PMD™18-T Vector Cloning Kit (TaKaRa) and then transformed into Trans 5α Chemically Competent Cells (TransGen) according to the manufacturer's instructions. M13 universal primers were used for sequencing, and every base was determined by sequencing at least four independent overlapping clones. Positive clones were selected, sequenced and analyzed with the DNAMAN program and the BLASTx program on the NCBI website.

RT-PCR amplifications were performed to determine the gap sequences between different clones. DsRNA-specific primers were designed based on the sequences obtained above. The detailed methods of the RT-PCR amplifications were as previously described (Wang et al., 2013; Xie et al., 2011). The mixtures of purified dsRNA as template and tagged random primer-dN6 were heat-denatured at 95 °C for 10 min and then immediately chilled on ice for 10 min. The mixtures were then reverse transcribed using Transcript™II One-Step gDNA Removal and cDNA Synthesis SuperMix (TransGen) at 50 °C for 2 h, and the enzyme then was inactivated at 85 °C for 10 min. The resulting cDNA products were used as the template for specific PCR amplification using 2 × TransTaq® High Fidelity (HiFi) PCR SuperMix (TransGen). The PCR products were purified, cloned and sequenced as described above.

To obtain the 3′ terminal sequence of dsRNA, a classic 3′-RACE (Rapid Amplification of cDNA Ends) protocol using an adaptor-linked oligo-dT primer was performed using the 3′-Full RACE Core Set Ver.2.0 (TaKaRa) according to the manufacturer's instructions. The 3′ RNA-ligase-mediated RACE (RLM-RACE) protocol was carried out to determine the 5′-terminal sequences of the coding strand of the dsRNA element (Xie et al., 2006; Chiba et al., 2009). All of the amplified cDNAs were cloned and sequenced as described above.

Sequence and phylogenetic analysis

The assembly and analysis of nucleotide sequences and translation of ORFs were performed using DNAMAN version 6 software. Potential

ORFs were found using the National Center for Biotechnology Information (NCBI) ORF Finder tool (http://www.ncbi.nlm.nih.gov/projects/gorf). The sequences of previously reported mycoviruses referenced in this paper were derived from the NCBI GenBank database (http://www.ncbi.nlm.nih.gov/genomes). Homology searches were performed using the NCBI Blast program (http://blast.st-va.ncbi.nlm.nih.gov/Blast.cgi). Potential secondary structures at the 5′-terminus were predicted using Mfold version 2.3 (http://mfold.rna.albany.edu/) (Zuker, 2003). The deduced amino acid sequences of the polyproteins or conserved domains were aligned using DNAMAN version 6 software with the default parameters (Katoh and Toh, 2008). The NJ trees were constructed using the neighbor-joining method of MEGA version 6 software with bootstrapping analysis of 1000 replicates. The best-fit model for a data set was chosen and maximum likelihood phylogenetic trees were constructed using MEGA 6 software. Branch support was determined by bootstrapping (1000 replicates).

Curing strain JS16 of virus

To identify the effects of the dsRNA element on strain JS16, four methods, including single conidial isolation, single ascospore isolation, protoplast-regenerant isolation and Ribavirin treatment, were used to eliminate the dsRNA segment from the host fungus. Conidiation was induced in CMC medium as previously described (Hou et al., 2002). The preparation of protoplasts was carried out as previously described (Hou et al., 2002). The carrot agar protocol for the production of perithecia and ascospores was described previously (Klittich and Leslie, 1988). Ribavirin is a nucleoside analog that induces mutations in RNA viral genomes and is useful to cure particular mycoviruses (Parker, 2005). Mycelial plugs of strain JS16 were cultured on PDA plates containing 80–100 μM of ribavirin at 25 °C for 4 d in the dark (Herrero and Zabalgogeazcoa, 2011). Then, hyphal tips were removed from the colony margin under a dissecting microscope, transferred onto a piece of cellulose membrane on a 60-mm-diameter PDA plate and grown at 25 °C for 5–7 d in the dark (Kanematsu et al., 2004). A combination method of protoplast-regenerant and Ribavirin treatment was also used to cure the virus from the host strain. The absence of viruses was determined using dsRNA extraction, RT-PCR, and northern blot.

Impact of the virus on the host biological properties

Mycelial growth, conidiation, virulence, biomass and mycotoxin production of strain JS16 and its virus-free strain JS16-F were assessed as previously described (Wang et al., 2013; Gale et al., 2002; Kang and Buchenauer, 1999; Bluhm et al., 2007; Seong et al., 2006)

Total RNA preparation and relative quantitative real-time RT-PCR

Mycelial plugs of strain JS16 and strain JS16-F were cultured on PDA plates overlaid with cellophane membranes for 36 h and 5 d, respectively, at 25 °C in the dark. The mycelial mass was collected and ground in liquid nitrogen with a mortar and pestle to a fine powder. Total RNAs were extracted with a Fungal RNA kit (OMEGA) according to the manufacturer's instructions, treated with DNase I (TaKaRa Bio Inc.) to completely remove genomic DNA, and suspended in DEPC-treated water. The synthesis of cDNAs was performed with M-MLV reverse transcriptase (Promega) and an oligo d (T) primer to quantify mRNA expression (Lee et al., 2014). Relative quantitative real-time RT-PCR (qRT-PCR) was performed on a CFX96 Real-Time PCR System (Bio-Rad, Herculess, U.S.A.) using the TransStart® Green qPCR SuperMix UDG (TransGen) according to the manufacturer's instructions. Two endogenous reference genes encoding cyclophilin 1 (CYP1, locus FGSG_07439) and elongation factor 1α (EF1α, locus FGSG_08811) were selected as reference genes to normalize the real time RT-PCR results (Lee et al., 2014). Another 9 *F. graminearum* genes that are predicted to be responsible for PTGS were selected (Lee et al., 2014). Of the 9 *F. graminearum* genes, 2 (FGSG_08752; are Argonaute-like genes, 2 (FGSG_09025; FGSG_04408) are Dicer-like genes, and 5 (FGSG_04619; FGSG_06504; FGSG_08716; FGSG_09076; FGSG_01582) are RdRP-like genes.

Data analysis

The data were subjected to analysis of variance (ANOVA) using the SAS® 8.0 program. The treatment means were compared using the least significant difference (LSD) test at the $p=0.01$ level. Each experiment included at least 3 replicates.

Acknowledgments

This work was supported by the National Natural Science Foundation of China (31171818). We thank Dr. Nobuhiro Suzuki for helpful suggestions about classification of the family *Hypoviridae* and FgHV2.

Appendix A. Supporting information

Supplementary data associated with this article can be found in the online version at http://dx.doi.org/10.1016/j.virol.2015.02.047.

References

Akhmedov, A.T., Gross, B., Jessberger, R., 1999. Mammalian SMC3 C-terminal and coiled-coil protein domains specifically bind palindromic DNA, do not block DNA ends, and prevent DNA bending. J. Biol. Chem. 274 (53), 38216–38224.
Bluhm, B.H., Zhao, X., Flaherty, J.E., Xu, J.R., Dunkle, L.D., 2007. RAS2 regulates growth and pathogenesis in *Fusarium graminearum*. Mol. Plant-Microbe Interact. 20, 627–636.
Chiba, S., Lin, Y.H., Kondo, H., Kanematsu, S., Suzuki, N., 2013. Effects of defective interfering RNA on symptom induction by, and replication of, a novel Partitivirus from a phytopathogenic fungus, *Rosellinia necatrix*. J. Virol. 87 (4), 2330–2341.
Chiba, S., Salaipeth, L., Lin, Y., Sasaki, A., Kanematsu, S., Suzuki, N., 2009. A novel bipartite double-stranded RNA mycovirus from the white root rot fungus *Rosellinia necatrix*: molecular and biological characterization, taxonomic considerations, and potential for biological control. J. Virol. 83, 12801–12812.
Chu, Y.M., Jeon, J.J., Yea, S.J., Kim, Y.H., Yun, S.H., Lee, Y.W., Kim, K.H., 2002. Double-stranded RNA mycovirus from *Fusarium graminearum*. App. Environ. Microbiol. 68, 2529–2534.
Darissa, O., Willingmann, P., Wilhelm, S., Adam, G., 2011. A novel double-stranded RNA mycovirus from *Fusarium graminearum*: nucleic acid sequence and genomicn structure. Arch. Virol. 156, 647–658.
Dawe, A.L., Nuss, D.L., 2013. Hypovirus molecular biology: from Koch's postulates to host self-recognition genes that restrict virus transmission. Adv. Virus Res. 86, 109–147.
Gale, L.R., Chen, L.F., Hernick, C.A., Takamura, K., Kistler, H.C., 2002. Population analysis of *Fusarium graminearum* from wheat fields in eastern China. Phytopathology 92, 1315–1322.
Ghabrial, S.A., Suzuki, N., 2009. Viruses of plant pathogenic fungi. Annu. Rev. Phytopathol. 47, 353–384.
Gossen, B.D., Rimmer, S.R., Holley, J.D., 2001. First report of resistance to benomyl fungicide in *Sclerotinia sclerotiorum*. Plant Dis. 85, 1206.
Haering, C.H., Lowe, J., Hochwagen, A., Nasmyth, K., 2002. Molecular architecture of SMC proteins and the yeast cohesin complex. Mol. Cell. 9 (4), 773–788.
Harvey, S.H., Krien, M.J., O'Connell, M.J., 2002. Structural maintenance of chromosomes (SMC) proteins, a family of conserved ATPases. Genome Biol. 3 (2), 3003.1–3003.5.
Herrero, N., Pérez-Sánchez, R., Oleaga, A., Zabalgogeazcoa, I., 2011. Tick pathogenicity, thermal tolerance and virus infection in *Tolypocladium cylindrosporum*. Ann. Appl. Biol. 159, 192–201.
Herrero, N., Zabalgogeazcoa, I., 2011. Mycoviruses infecting the endophytic and entomopathogenic fungus *Tolypocladium cylindrosporum*. Virus Res. 160, 409–413.
Hillman, B.I., Foglia, R., Yuan, W., 2000. Satellite and defective RNAs of Cryphonectria hypovirus 3-grand haven 2, a virus species in the family *Hypoviridae* with a single open reading frame. Virology 276, 181–189.
Hillman, B.I., Halpern, B.T., Brown, M.P., 1994. A viral dsRNA element of the chestnut blight fungus with a distinct genetic organization. Virology 201, 241–250.

Hillman, B.I., Shapira, R., Nuss, D.L., 1990. Hypovirulence-associated suppression of host functions in *Cryphonectria parasitica* can be partially relieved by high light intensity. Phytopathology 80, 950–956.
Hillman, B.I., Suzuki, N., 2004. Viruses of the chestnut blight fungus, *Cryphonectria parasitica*. Adv. Virus Res. 63, 423–472.
Hillman, B.I., Tian, Y., Bedker, P.J., Brown, M.P., 1992. A North American hypovirulent isolate of the chestnut blight fungus with European isolate-related dsRNA. J. Gen. Virol. 73, 681–686.
Hirano, T., 2006. At the heart of the chromosome: SMC proteins in action. Nat. Rev. Mol. Cell Biol. 7, 311–322.
Hou, Z., Xue, C., Peng, Y., Katan, T., Kistler, H.C., Xu, J., 2002. A mitogen-activated protein kinase gene (MGV1) in *Fusarium graminearum* is required for female fertility, heterokaryon formation, and plant infection. Mol. Plant Microbe Interact. 15, 1119–1127.
Hu, Z., Wu, S., Cheng, J., Fu, Y., Jiang, D., Xie, J., 2014. Molecular characterization of two positive-strand RNA viruses co-infecting a hypovirulent strain of *Sclerotinia sclerotiorum*. Virology 464–465, 450–459.
Jensen, R.B., Shapiro, L., 2003. Cell-cycle-regulated expression and subcellular localization of the *Caulobacter crescentus* SMC chromosome structural protein. J. Bacteriol. 185 (10), 3068–3075.
Kanematsu, S., Arakaw, M., Oikawa, Y., Onoue, M., Osaki, H., Nakamura, H., Ikeda, K., Kuga-Uetake, Y., Nitta, H., Sasaki, A., Suzaki, K., Yoshida, K., Matsumoto, N., 2004. A reovirus causes hypovirulence of *Rosellinia necatrix*. Phytopathology 94, 561–568.
Kang, Z., Buchenauer, H., 1999. Immunocytochemical localization of *fusarium* toxins in infected wheat spikes by *Fusarium culmorum*. Physiol. Mol. Plant Pathol. 55, 275–288.
Katoh, K., Toh, H., 2008. Recent developments in the MAFFT multiple sequence alignment program. Brief. Bioinform. 9, 286–298.
Khalifa, M.E., Pearson, M.N., 2014. Characterisation of a novel hypovirus from *Sclerotinia sclerotiorum* potentially representing a new genus within the *Hypoviridae*. Virology 464–465, 441–449.
King, A.M.Q., Adams, M.J., Carstens, E.B., Lefkowitz, E.J., 2012. Virus Taxonomy: Classification and Nomenclature of Viruses. Ninth Report of the International Committee on Taxonomy of Viruses. Elsevier Academic Press, London, UK.
Klittich, C., Leslie, J.F., 1988. Nitrate reduction mutants of *Fusarium Moniliforme* (*Gibberella Fujikuroi*). Genetics 118, 417–423.
Koloniuk, I., El-Habbak, M.H., Petrzik, K., Ghabrial, S.A., 2014. Complete genome sequence of a novel hypovirus infecting *Phomopsis longicolla*. Arch. Virol. 159 (7), 1861–1863.
Koonin, E.V., Choi, G.H., Nuss, D.L., Shapira, R., Carrington, J.C., 1991. Evidence for common ancestry of a chestnut blight hypovirulence associated double-stranded RNA and a group of positive-strand RNA plant viruses. Proc. Natl Acad. Sci. USA 88, 10647–10651.
Kuang, J., Wang, J., Zhou, M., 2011. Monitoring on carbendazim and dimethachlon-resistance of *Sclerotinia sclerotiorum* obtained from the blight stems of rape in Jiangsu Province. Chin. Agric. Sci. Bull. 27 (15), 285–291.
Laflamme, G., Tremblay-Boudreault, T., Roy, M.A., Andersen, P., Bonneil, E., Atchia, K., Thibault, P.D., Amours, D., Kwok, B.H., 2014. Structural maintenance of chromosome (SMC) proteins link microtubule stability to genome integrity. J. Biol. Chem. 289, 27418–27431.
Lee, K.M., Cho, W.K., Yu, J., Son, M., Choi, H., Min, K., Lee, Y.W., Kim, K.H., 2014. A comparison of transcriptional patterns and mycological phenotypes following infection of *Fusarium graminearum* by four mycoviruses. PLoS One 9 (6), e100989.
Linder-Basso, D., Dynek, J.N., Hillman, B.I., 2005. Genome analysis of Cryphonectria hypovirus 4, the most common hypovirus species in North America. Virology 33, 192–203.
Luo, Y., Deng, X.F., Cheng, F., Li, Y., Qiu, J.M., 2013. SMC1-mediated intra-S-phase arrest facilitates *Bocavirus* DNA replication. J. Virol. 87, 4017–4032.
Ma, H., Feng, X., Chen, Y., Chen, C., Zhou, M., 2009. Occurrence and characterization of dimethachlon insensitivity in *Sclerotinia sclerotiorum* in Jiangsu Province of China. Plant Dis. 93, 36–42.
Martin, D.P., Lemey, P., Lott, M., Moulton, V., Posada, D., Lefeuvre, P., 2010. RDP3: a flexible and fast computer program for analyzing recombination. Bioinformatics 26, 2462–2463.
McMullen, M., Jones, R., Gallenberg, D., 1997. Scab of wheat and barley: a re-emerging disease of devastating impact. Plant Dis. 81, 1340–1348.
Mu, R., Romero, T.A., Hanley, K.A., Dawe, A.L., 2011. Conserved and variable structural elements in the 5′ untranslated region of two hypoviruses from the filamentous fungus *Cryphonectria parasitica*. Virus Res. 161, 203–208.
Nuss, D.L., 2005. Hypovirulence: mycoviruses at the fungal-plant interface. Nat. Rev. Microbiol. 3, 632–642.
O'Donnell, K., Kistler, H.C., Tacke, B.K., Casper, H.H., 2000. Gene genealogies reveal global phylogeographic structure and reproductive isolation among lineages of *Fusarium graminearum*, the fungus causing wheat scab. Proc. Natl Acad. Sci. USA 97, 7905–7910.
Parker, W.B., 2005. Metabolism and antiviral activity of ribavirin. Virus Res. 107, 165–171.
Perera, O.P., Snodgrass, G.L., Allen, K.C., Jackson, R.E., Becnel, J.J., O'Leary, P.F., Luttrell, R.G., 2012. The complete genome sequence of a single-stranded RNA virus from the tarnished plant bug, *Lygus lineolaris* (Palisot de Beauvois). J. Invertebr. Pathol. 109, 11–19.
Rocha, O., Ansari, K., Doohan, F.M., 2005. Effects of trichothecene mycotoxins on eukaryotic cells: a review. Food Addit. Contam. 22, 369–378.
Segers, G.C., Zhang, X, Deng, F, Sun, Q, Nuss, D.L., 2007. Evidence that RNA silencing functions as an antiviral defense mechanism in fungi. Proc. Natl. Acad. Sci. USA 104, 12902–12906.
Seong, K., Li, L., Hou, Z.M., Tracy, M., Kistler, H.C., Xu, J.R., 2006. Cryptic promoter activity in the coding region of the HMG-CoA reductase gene in *Fusarium graminearum*. Fungal Genet. Biol. 43, 34–41.
Shapira, R., Choi, G.H., Hillman, B.I., Nuss, D.L., 1991. The contribution of defective RNAs to the complexity of viral-encoded double-stranded RNA populations present in hypovirulent strains of the chestnut blight fungus *Cryphonectria parasitica*. EMBO J. 10, 741–746.
Smart, C.D., Yuan, W., Foglia, R., Nuss, D.L., Fulbright, D.W., Hillman, B.I., 1999. Cryphonectria hypovirus 3, a virus species in the family *Hypoviridae* with a single open reading frame. Virology 265, 66–73.
Soppa, J., Kobayashi, K., Noirot-Gros, M.F., Oesterhelt, D., Ehrlich, S.D., Dervyn, E., Ogasawara, N., Moriya, S., 2002. Discovery of two novel families of proteins that are proposed to interact with prokaryotic SMC proteins, and characterization of the *Bacillus subtilis* family members ScpA and ScpB. Mol. Microbiol. 45 (1), 59–71.
Sun, Q, Choi, G.H., Nuss, D.L., 2009. A single Argonaute gene is required for induction of RNA silencing antiviral defense and promotes viral RNA recombination. Proc. Natl. Acad. Sci. USA 106, 17927–17932.
Suzuki, N., Maruyama, K., Moriyama, M., Nuss, D.L., 2003. Hypovirus papain-like protease p29 functions in trans to enhance viral double stranded RNA accumulation and vertical transmission. J. Virol. 77, 11697–11707.
Theisen, S., Roeseler, S., Berger, S., Buchenauer, H., 2001. Analysis of double-stranded RNA and virus-like particles in trichothecene-producing strains of *Fusarium graminearum*. Mycotoxin Res. 17, 32–36.
Valverde, R.A., 1990. Analysis of double-stranded RNA for plant virus diagnosis. Plant Dis. 74, 255–258.
Wang, S., Kondo, H., Liu, L., Guo, L., Qiu, D., 2013. Anovel virus in the family *Hypoviridae* from the plant pathogenic fungus *Fusarium graminearum*. Virus Res. 174, 69–77.
Windels, C.E., 2000. Economic and social impacts of fusarium head blight: changing farms and rural communities in the northern great plains. Phytopathology 90 (1), 17–21.
Xie, J., Wei, D., Jiang, D., Fu, Y., Li, G., Ghabrial, S.A., Peng, Y., 2006. Characterization of debilitation-associated mycovirus infecting the plant-pathogenic fungus *Sclerotinia sclerotiorum*. J. Gen. Virol. 87, 241–249.
Xie, J., Xiao, X., Fu, Y., Liu, H., Cheng, J., Ghabrial, S.A., Li, G., Jiang, D., 2011. A novel mycovirus closely related to hypoviruses that infects the plant pathogenic fungus *Sclerotinia sclerotiorum*. Virology 418, 49–56.
Yaegashi, H., Kanematsu, S., Ito, T., 2012. Molecular characterization of a new hypovirus infecting a phytopathogenic fungus, *Valsa ceratosperma*. Virus Res. 165, , 143–150.
Yu, J., Kwon, S.J., Lee, K.M., Son, M., Kim, K.H., 2009. Complete nucleotide sequence of double-stranded RNA viruses from *Fusarium graminearum* strain DK3. Arch. Virol. 154, 1855–1858.
Yu, X., Li, B., Fu, Y., Jiang, D., Ghabrial, S.A., Li, G., Peng, Y., Xie, J., Cheng, J., Huang, J., Yi, X., 2010. Ageminivirus-related DNA mycovirus that confers hypovirulence to a plant pathogenic fungus. Proc. Natl. Acad. Sci. USA 107, 8387–8392.
Yuan, W., Hillman, B.I., 2001. In vitro translational analysis of genomic, defective, and satellite RNAs of Cryphonectria hypovirus3-GH2. Virology 281, 117–123.
Zhang, X, Nuss, D.L., 2008. A host Dicer is required for defective viral RNA production and recombinant virus vector RNA instability for a positive sense RNA virus. Proc. Natl. Acad. Sci. USA 105, 16749–16754.
Zhang, X, Segers, G.C., Sun, Q, Deng, F, Nuss, D.L., 2008. Characterization of hypovirus-derived small RNAs generated in the chestnut blight fungus by an inducible DCL-2-dependent pathway. J. Virol. 82, 2613–2619.
Zhang, D., Spiering, M.J., Nuss, D.L., 2014. Characterizing the roles of *Cryphonectria parasitica* RNA-dependent RNA polymerase-like genes in antiviral defense, viral recombination and transposon transcript accumulation. PLoS One 9 (9), e108653.
Zuker, M., 2003. Mfold web server for nucleic acid folding and hybridization prediction. Nucl. Acids Res. 31, 3406–3415.